Building and Environment 249 (2024) 111123

Contents lists available at ScienceDirect

Building and Environment

journal homepage: www.elsevier.com/locate/buildenv

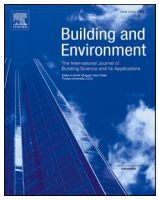

Review of adaptive opaque façades and laboratory tests for the dynamic thermal performance characterization

Miren Juaristi [a,*], Moncef Krarti [b]

[a] Institute for Renewable Energy, EURAC Research, Viale Druso 1, Bolzano, 39100, Italy
[b] Building Systems Program, Civil, Environmental and Architectural Engineering Department, University of Colorado, Boulder, 80309, CO, United States

ARTICLE INFO

Keywords:
Thermal characterization
Building envelope
Experimental testing protocols
Dynamic insulation
Thermal transmittance
Thermal resistance

ABSTRACT

Adaptive opaque facades can dynamically adapt their thermal properties according to both outdoor and indoor conditions, hence can enhance the energy efficiency of the building while maintaining high indoor environmental quality. Traditional façade thermal performance metrics such as U-value or R-value can be useful to evaluate the energy performance of buildings. However, the adaptive opaque façade systems require versatile testing protocols to characterize their thermal performance under their various operation modes. This paper provides a comprehensive review the experimental testing protocols and standards that have been reported to characterize the dynamic thermal performance of adaptive opaque façades. These testing protocols are compared to those commonly used to evaluate conventional building envelope assemblies. The outcomes of the review include a set of recommendations to develop laboratory testing set-ups, protocols, and metrics to consistently measure the dynamic thermal performance of adaptive opaque facades.

1. Introduction

1.1. Background & research gap

To address the urgent need of reducing energy consumption of buildings, development of advanced envelope technologies is becoming one of the cornerstones of energy efficiency and sustainability for the built environment [1]. Indeed, opaque façade systems have incrementally evolved in the last few decades to have higher thermal resistance and lower air leakage as a passive solution to reduce the energy need for space heating and cooling and therefore to achieve the Zero Energy Building Target [2]. However, as evidenced by several reported research studies, envelope elements with high thermal resistance are not always beneficial to optimize the thermal performance of buildings and to effectively reduce thermal heating and cooling loads and ultimately energy demands [3,4]. Indeed, releasing indoor thermal heat gains during certain cooling demand periods and harvesting solar heat gains during heating demand periods through the building envelope can reduce the operational energy needs of buildings, and in some cases eliminate the need for any active heating and cooling systems. According to some reported analyses, the annual heating and cooling energy demands could be reduced by up to 69% if thermal properties of opaque building envelopes are dynamically adjusted and properly controlled to account for climatic conditions and building characteristics [5]. The building facades that are capable to adjust their thermal properties are often called adaptive facades [6]. Adaptive facades respond dynamically to changing conditions and requirements with the objective of reducing the energy consumption of buildings while guaranteeing comfortable indoor conditions [7]. The term adaptive facades should not be confused with facades integrating heating [8] and cooling systems [9], which operate and change indoor environmental characteristics using an energy input [10]. One specific category of adaptive facades consists of adaptive opaque facades, which can be used to control dynamically heat transfer between the outdoor and indoor environments [11]. The high energy efficiency potentials of these adaptive opaque facades have been highlighted by the several review analyses reported since 2018. These reviews focus on different technologies, such as dynamic/switchable thermal insulation technologies [12–14], parietodynamic and permeodynamic walls [15], phase change materials [16] and trombe walls [17–23]. A more general review has reported materials and elements that could be used to build adaptive opaque facades [11]. The main focus of the previously reported review analyses is to describe the investigated adaptive façade technology concepts and their operation mechanisms. One of the identified significant challenges is to be able to consider the performance of adaptive facades as part of intelligent

* Corresponding author.
E-mail address: miren.juaristigutierrez@eurac.edu (M. Juaristi).

https://doi.org/10.1016/j.buildenv.2023.111123
Received 29 August 2023; Received in revised form 24 November 2023; Accepted 17 December 2023
Available online 20 December 2023

Nomenclature

Abbreviations

PCM	Phase Change Material
PV	Photovoltaics
BIPV	Building Integrated Photovoltaics
BIPVT	Building-Integrated Photovoltaic-Thermal

Symbols

R_u	Overall Thermal Resistance
U	Thermal Transmittance or Overall Coefficient of Heat Transfer
C	Thermal Conductance
h_{env}	Surface coefficient of heat transfer
t_s	Surface temperature
T_{env}	Effective environmental temperature
R_{si}	Interior surface thermal resistance
R_{se}	Exterior surface thermal resistance
β	Temperature Rise Coefficient
T_z	Solar air temperature
E	Emissivity factor
h_r	Radiation coefficient
h_c	Convection coefficient
T'_r	Mean radiant temperature
DF	Decrement factor
TL	Time Lag
T_{in}	Indoor air temperature
T_{out}	Outdoor air temperature
T_c	Temperature of the pipe's section

buildings [24]. To avoid sub-optimization, adaptive façades and active systems should be coupled with the overall building performance, as they do other advanced envelope systems [17]. However, to do so, comprehensive indicators and performance tests are needed, essentials to understand the impact of adaptive facades in building energy savings and indoor comfort [24,25]. Fig. 1 summarizes the reported thermal performance metrics by cited review papers.

Equivalent R-values and/or U-values (thermal transmittance and thermal resistance, respectively) are commonly used to assess through simplified simulation models the impacts of opaque façade technologies when integrated at the building level. These performance metrics are compatible with RC-thermal network [26–31], and EnergyPlus software, either by using "Surface Control:Movable Insulation" [32], class list or "Material:AirGap" 33 coupled with Energy Management System' (EMS).

Most of the reported values regarding R-values and/or U-values of specific adaptive opaque façade technologies are not based on experimental testing analyses either under laboratory or field conditions (Fig. 2).

Measured thermal performance metrics have been reported extensively for adaptive facades consisting of airflow based dynamic walls, Trombe Walls [34], Parietodynamic walls, Permeodynamic walls [11,13,15] and Double-Skin Facades [14,16]. Building envelope systems integrated with Phase Change Materials (PCMs) have also been widely tested as reported by several review analyses [14,35,36]. Regarding Dynamic Insulations, some transparent Dynamic Insulations have also been evaluated and characterized through experimental testing as identified in the literature reviews [14,15].

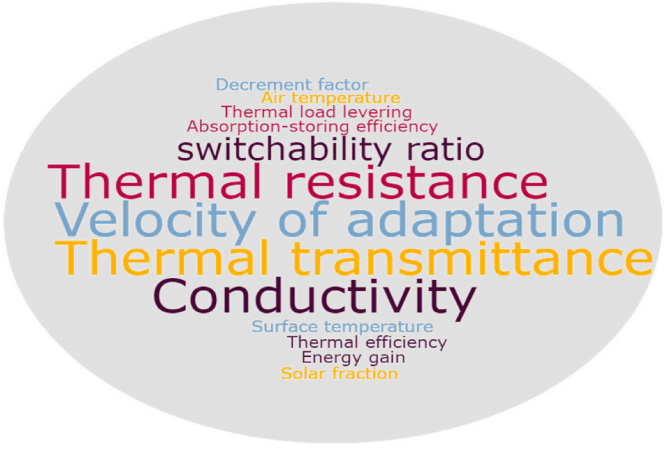

Fig. 1. Thermal performance metrics reported by previously reported literature reviews.

The main research gap of the reported review analyses is the lack of characterization of the dynamic thermal performance of opaque adaptive façades using repeatable experimental tests excluding airflow based dynamic walls which have been tested more widely. As summarized in Fig. 2, previous review papers were mostly focused on explaining the working principles of the different technologies. Limited studies have described and performed measurements of adaptive opaque facades. The few review analyses that have reported thermal performance metrics obtained through laboratory testing have not described the characterization methods and testing procedures in detail. Moreover, there is a lack of common approaches and guidelines for testing procedures among the reported studies. Well defined testing protocols are essential to compare the thermal performance of adaptive building envelope systems fairly and effectively, and ultimately increase their improvement and adoption.

1.2. Research aim & objectives

The main goal of this review paper is to identify effective experimental setups and universal testing protocols for assessing the dynamic thermal performance of adaptive opaque façades. First, the main differences in testing the thermal performance between conventional static wall assemblies and adaptive opaque façades are highlighted. Then, reported testing approaches and protocols specific to adaptive opaque facades are described.

The outcome of the critical review conducted in this paper is to establish criteria and guidelines required to experimentally test the dynamic thermal performance of adaptive opaque facades, including (i) testing set-up descriptions, (ii) measurable parameters and performance metrics and (iii) testing protocols. To establish this novel set of criteria, first Section 2 outlines existing protocols and standards for the thermal characterization of opaque facades. Section 3 reviews scientific papers where the protocols are adapted for the dynamic thermal performance characterization. In Section 4, the performance tests of adaptive opaque façade components are reviewed.

1.3. Research methods & scope

The scientific literature review was performed by using google scholar search engine. Table 1 summarizes the adopted methodology and searched information and features for the review analysis.

The critical review presented in this paper focuses only on the opaque façade systems that can involve variable convective and conductive heat transfer mechanisms, i.e., dynamic insulation systems and controllable air cavities. These façade systems can have common experimental testing protocols. Thus, the paper excludes any façades that involve air-flow exchanges between the indoors and outdoors as the

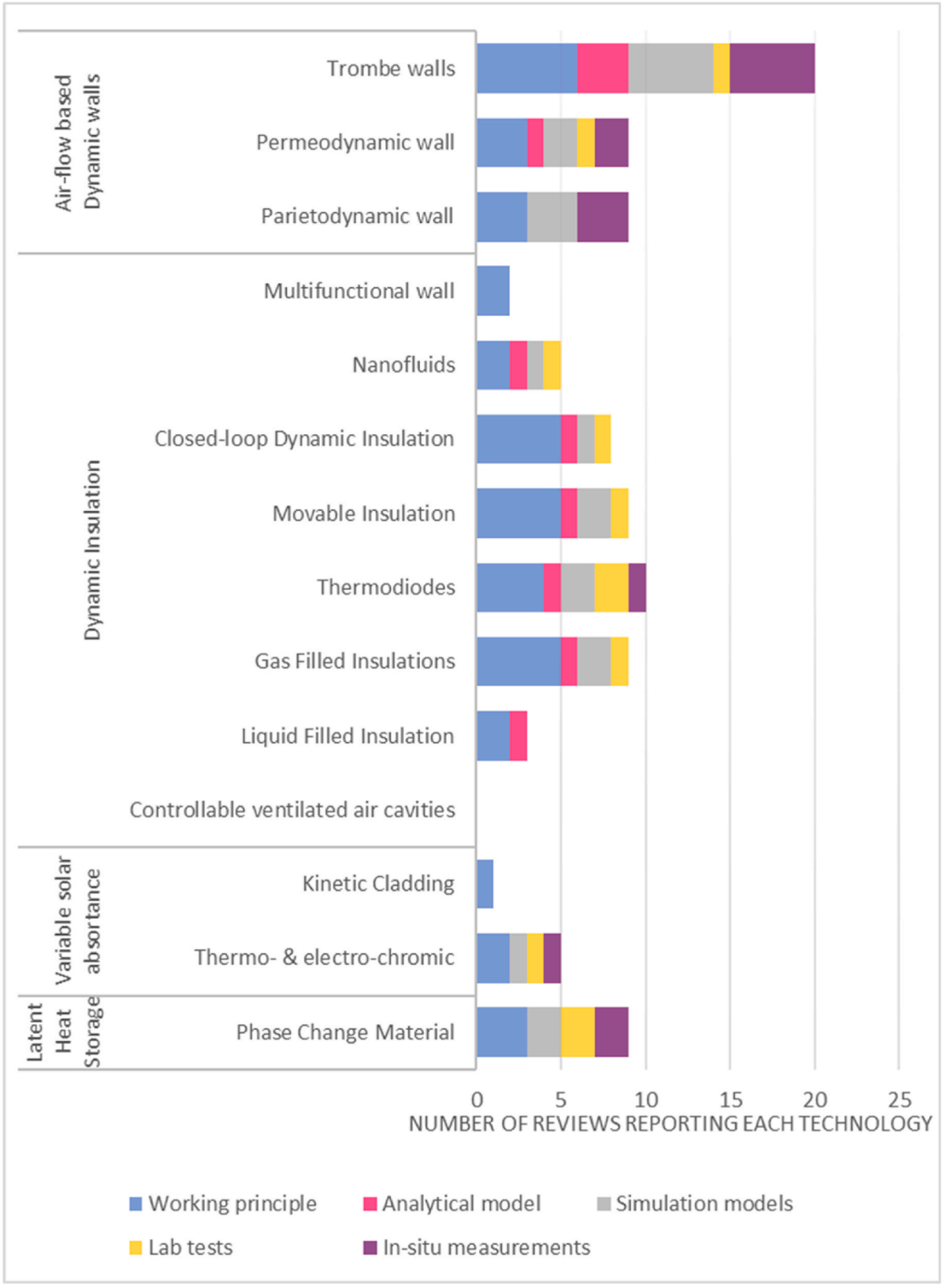

Fig. 2. Number of review papers reporting testing methods for dynamic thermal characterization of adaptive opaque facades.

performance of these systems require different testing protocols. Since the thermal performance of facades integrating phase change materials (PCMs) have been widely characterized through experimental testing, reported testing analyses will be summarized as part of this review to highlight any possible guidelines applicable to adaptive opaque façades.

2. Existing standards and testing protocols to characterize in laboratory the thermal performance of opaque façade components

The thermal characterization of building envelope façades through

Table 1
Methodology of the scientific review.

Keywords	Inclusion & exclusion Criteria	Searched information and features
• "Adaptive opaque facades" •"Dynamic insulation" •"Active insulation •"Dynamic insulation review" •"Trombe walls •"Hot box, solar" •"Hot box, dynamic" •"Hot box, thermal mass" •"Hot box, air cavity" •"Hot box, radiation"	•Literature reviews from 2018 to 2023 •Papers with experimental tests details o No constraints on publication dates o Excluding facades involving air-flow exchange between the indoor and outdoor environments •No constraints on publication dates	•Followed testing protocols and standards • •Characteristics of the experimental set ups including testing facilities and applicable specimens •Testing methods (i.e., sensors placement, boundary conditions and validity criteria) •Measured parameters

experimental testing is crucial to validate numerical or analytical models, as well as to better understand the thermal behavior of building shell. Soares et al. have reviewed the main methodologies for measuring the overall thermal transmittance of homogeneous elements, moderately homogeneous and non-homogeneous walls, windows, and some innovative construction elements such as aerogel, PCMs and vacuum insulation panels [37]. They compared the heat flow meter method used by ISO 9869 [38] and 8301 [39], the guarded hot plate [40], the hot box (considering the guarded and the calibrated) described both in ISO 8890 [41] and ASTM C1363-19 [42] and the infrared thermography adopted by the British Standards Institution [43], ISO 10878 [44] and ISO 9869 [45]. However, the review analysis did not consider specifically the characterization of adaptive opaque façade Systems beyond those integrating PCMs. This review points out that guarded hot plate set-up is limited to low conductivity materials of relatively small-scale samples, so tests of large façade systems cannot be adequately performed. To apply the infrared thermography method to test lightweight and super-insulated walls, more research and development is needed. Indeed, according to a review analysis specific to infrared thermography [46], this method does not currently provide reliable results for wall assemblies with air gaps. Thus, adaptive opaque façade systems could be tested using either guarded or calibrated hot box apparatuses (Fig. 3). Both apparatuses include one cold chamber and one hot chamber, which integrates a heating input system through a metered box. For the guarded hot box, the hot chamber consists of a metering box and a guard box, in which the indoor environment is controlled. This minimizes lateral heat flow during the experimental testing and ensure that the total heat flow through the specimen is equal to the heat input to the metering box. In the calibrated hot box, the hot chamber consists of only the metering box surrounded by temperature-controlled spaces, which are not necessarily set at the same air temperature as that inside the metering box. In this case, the total power input shall be corrected for the wall and flanking effects.

There are two standards for testing the thermal properties of building envelope systems which define the experiment procedures, the specifications of the measuring apparatus, and their calibration requirements. These standards include ISO 8990 [41] and ASTM C1363 [42]. These standards allow some flexibilities and do not mandate specific design or size for the testing apparatus. Some configurations of modified hot box experimental set-up have been proposed including those integrated with measurement and control systems [47]. Using calibrated and hot box apparatuses, large and inhomogeneous building envelope specimens can be tested under complex boundary conditions, involving not only temperature differences, but also variations in air velocity and relative humidity. The effects of the heat direction can be measured using these apparatuses for wall (horizontal heat flow) and floor (vertical heat flow) configurations. Both ISO and ASTM standards enable the determination of the thermal properties for the tested specimen as summarized in Table 2.

For highly inhomogeneous building envelope systems, only an overall thermal resistance [R_u] or transmittance [U] can be measured, as the heat transfer can vary significantly spatially along the specimen surface making accurate measurement of the average surface temperatures difficult to achieve. In these cases, the tested specimen should be of the same thickness as the actual building envelope systems [42]. ISO 8990 defines inhomogeneous specimens as those having local differences in surface temperatures which exceed 20% of the mean surface-to-surface temperature difference. For slightly inhomogeneous specimens, the ISO and ASTM standards provide calculation methods for the environmental temperatures, whether the convection coefficient is known and not, as summarized in Table 3.

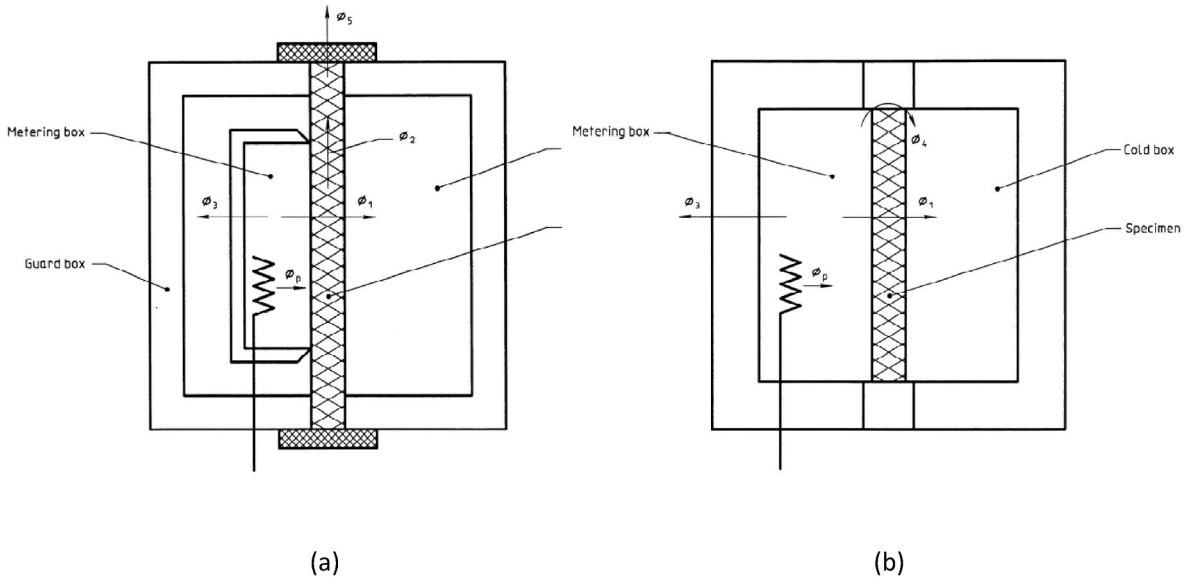

Fig. 3. Guarded hot box set-up (a) and calibrated hot box set-up (b). Source [41].

Table 2
Calculated thermal characteristics and parameters that need to be measured.

Measurable properties	Units	Specimen Types	Applicable Equations	Measurable parameters	Fixed parameters
Overall Thermal Resistance	m^2K/W	Homogenous, non-very inhomogenous and very inhomogenous	$R_u = \frac{A\,(T_{env,i} - T_{env,e})}{Q}$ $R_u = R_{env,i} + R + R_{env,e}$	Thermal flux through the specimen [Q], surface temperature [T_1, T_2], air temperatures and radiant temperatures	Radiation coefficient and convection coefficient
Thermal Transmittance, also called as Overall Coefficient of Heat Transfer [U]	W/m^2K	Homogenous, non-very inhomogenous and very inhomogenous	$U = \frac{Q}{A\,(T_{env,i} - T_{env,e})}$ $U = h_{env,i} + C + h_{env,e}$		
Thermal Conductance [C]	W/m^2K	Homogenous and non-very inhomogenous	$C = \frac{Q}{A\,(T_1 - T_2)}$	Thermal flux through the specimen [Q], surface temperature [T_1, T_2]	–

None of the available standards provide simplified performance metrics for different scenarios of natural and forced ventilation and radiation coefficients, which determine the Effective Environmental temperatures (T_{env}). Thus, surface heat transfer coefficients can only be estimated by using standard of equal thermal resistance, size, surface configuration and roughness if geometry, average temperatures, and energy exchange conditions are similar for the reference and tested specimens [42]. As demonstrated by a reported literature review which compares experimental data and conventional values provided by ISO6946 [48], the influence of environmental boundary conditions on surface thermal resistances is not properly captured by the simplified calculation methods. Thus, and as advised by the standard, it is highly recommended to specify the testing boundary conditions when reporting measured values for the overall thermal resistances. ASTM C1363 standard also highlights that for specimens containing closed cavities or cavities open to one surface, the overall thermal resistances or transmittances could depend on the temperature differences across the tested specimens due to internal convection heat transfer. Therefore, boundary conditions for these types of specimens need to be selected carefully and reported with the measured performance properties. Moreover, for vertical specimens with air spaces that significantly affect thermal performance, the dimensions of the metering chamber should match the effective construction height. Finally, placement of temperature sensors could affect measurements and needs to be elected depending on the type of convection heat transfer (i.e., natural or forced) prevalent in the tested specimens.

The main differences between both standards are the validity requirements as well as the experimental set up specifications as summarized in Table 4.

The scope of these standards does not include the thermal characterization of the building envelope components that intentionally involve fluid flows through them (air or water). For these types of facades, the test procedures need to be revised as indicated for facades that are permeable to moisture [49], trombe walls [34], permeodynamic walls [50], and parietodynamic walls. For parietodynamic walls, the mass flow between environment has been measured with anemometers [51,52] and with rotameters [53]. For walls subject to water flows, it is essential to control and monitor the relative humidity variations. For facades involving any kind of fluid exchanges, heat balances need to account for fluid flows through the specimens [49].

The test methods summarized in Table 4 applies to steady-state testing and does not specify procedures or guidelines for conducting dynamic tests suitable for adaptive facades. However, there are reported testing experiences for measuring dynamic performance of building envelope systems. These tests have been reviewed and discussed in Section 3.

2.1. Review of experimental tests characterizing the performance of opaque façade components in steady-state regime: research scope from 2018 to 2023

The standards outlined in the previous section are well established and have been used for decades to measure the thermal performance of non-homogenous building envelope systems under steady-state conditions. However, applications of Guarded Hot Box and Calibrated Hot Box apparatuses have provided significant insights on their advantages and

Table 3
Calculation of the environmental temperatures for each standard.

Standard	Measurable property	Unit	Applicable Equation	Coefficient values set by the standard
ASTM C1363	Surface coefficient of heat transfer	W/m^2K	$h_{env} = \frac{Q}{A\,(T_{env} - T_1)}$ (1)	None
	Temperature difference between average test specimen surface and effective environmental temperature	K	$\Delta t_{s-env} = \frac{h_c \bullet \Delta T_{s-a} + h_r \bullet \Delta T_{s-b}}{h_r + h_c}$ (2)	
ISO 8990	Surface thermal resistance	m^2K/W	$R_s = \frac{1}{Eh_r + h_c}$ (3)	$h_r = 4\sigma T_m^3$ $h_c = 3$ W/(m^2K) for natural convection at vertical surface. For non-uniform specimen, h_c cannot be calculated as requires the knowledge of mean surface temperature. In these cases, h_c can be estimated from the data during test on another uniform specimen can be taken
	Effective Environmental Temperature	K	$T_{env} = \frac{Eh_r}{Eh_r + h_c} T_r^{'} + \frac{h_c}{Eh_r + h_c} T_a$ (4)	

Being T'_r mean radiant temperature seen by the specimen; T_a, T_b temperature adjacent to specimen for each side; T_m mean radiant absolute temperature; h_r radiation coefficient; h_c convection coefficient, E emissivity factor of the hot box.

Table 4
Differences in testing settings between ISO 8990 and ASTM C1363.

Standard	ISO 8990	ASTM C1363
Validity of measurements	The results of two successive measuring periods do not change more than 1%.	Equilibrium conditions are reached for at least 30 min (average metering box ambient air temperatures do not vary by more than + -0.25 °C). Tests are repeated in five-time constant blocks. The thermal transmittance calculated from the data of the five blocks do not vary more than + -2%.
Minimum number of sensors	At least two per square meter and not less than nine unless other information on temperature distribution is available. Supplementary sensors shall be applied to each region of varying temperature.	At least five thermocouple pairs pe square meter of the metering box unless a Heat Flux Transducer is placed on the metering chamber walls,
Chambers' temperature	Not pre-established, but close to the end conditions. Mean temperatures of 10 °C to 20 °C and difference of at least 20 °C are common in building applications.	Between −48 and 85 °C in the chamber representing the outside environment and 21 °C inside
Air velocity	For natural ventilation between 0.1 m/s to 10 m/s advisable	Velocities in the outdoor environment should be minimum and air velocities greater than 1 m/s are permissible when their effect upon heat transfer is to be determined. In these cases, 2.75 m/s for summer conditions and 5.5 m/s for winter conditions. When the effect of natural ventilation is not evaluated, suggestion of 0.3 m/s velocity for walls which are 3-m height, as a tradeoff between desired uniformity of the air curtain temperatures and the operational mode of convective flow.

limitations [37]. Indeed, the testing standards have been used to evaluate the effects of inhomogeneity for various building envelope façades including historic masonry walls [54] sawdust concrete masonry walls [55], lightweight steel framed wall [56], wood based framed walls [57], and ventilated face systems [58]. Moreover, the testing standards have been applied to assess the thermal performance of innovative systems made of biobased and recycled materials such as mortars made of re-used fly-ash and bottom ash [59], 3D-printed block filled with different recycled insulation materials [60], insulation boards containing foam-encapsulated vacuum insulation panels [61], risk husk panels [62], precast hemp concrete panels [63]. In some cases, the characterization of the thermal performance enabled a wider Life Cycle Assessment of the tested building envelope systems [62].

3. Experimental tests characterizing the dynamic performance of non-adaptive opaque façade components

The standards described in Section 2 were conceived to perform testing under steady-state conditions. However, opaque façade components, even static, do not always have the same behavior since they are exposed to dynamic boundary conditions that vary with time. In particular, the effects of thermal mass or latent heat storage can only be assessed through testing protocols carried out using dynamic conditions.

As highlighted by a reported review specific to thermal inertia in buildings [64] hot box set-up can be used for evaluating the thermal mass effects of building envelope systems. One of first tests of building envelope systems under dynamic conditions was reported in 2002 [65]. This test has been based on modifications of the existing standards to measure decrement factors and time lags for walls with high thermal inertia. The decrement factor (DF) is defined as the ratio of the amplitudes of outside and inside surface temperatures when the indoor air temperature is set to be constant as indicated by Equation (5).

$$DF = \frac{T_{in\ max} - T_{in\ min}}{T_{out\ max} - T_{out\ min}} \tag{5}$$

The time lag (TL) expresses the temporal difference between the peak temperature of wall's outside and inside surface temperatures for a constant indoor air temperature as defined by Equation (6).

$$TL = t_{Tin\ max} - t_{Tout\ max} \tag{6}$$

For this dynamic testing protocol, sinusoidal time variations of temperatures have been imposed for one day (i.e., 24-h period). Using this dynamic temperature variation, the thermal performance of 6 different walls, 2 traditional concrete walls and 4 walls with an innovative insulation material have been tested [66]. The guarded hot-box unit coupled with dynamic temperature variation has been used to determine response factors of walls [67,68], as well as thermal transmittances and decrement factors for façade systems [64,66]. Sinusoidal temperature variations using one-day period are not the only option to impose dynamic boundary conditions [69]. Time variations of temperature using one week cycle have been also considered to test the thermal performance of four different wood wall specimens [70]. The use of hot box apparatus results in more accurate estimation of thermal properties of building envelope assemblies than other testing procedures under dynamic boundary conditions [64,70].

The effects of integrating PCMs in walls have been widely measured using hot box apparatus under dynamic regimes [], including PCMs integrated in composites [71], microencapsulated in polyurethane foams [72] textile reinforced concrete panels [73] or filled in hollow bricks [74]. The most complex experiment consisted of a PCM encapsulated within a solar air heat exchanger having a ventilated air cavity [75]. For this system, the hot box apparatus has been coupled with artificial sun to replicate more realistic boundary conditions that account for the effects of solar radiation. Currently, the artificial sun is mostly used to test the thermal and optical performance of transparent façades (i.e., continuous fenestrated panels and windows) to ensure uniform distribution of solar irradiance [76]. The artificial sun is also used to test the thermal and electrical performance of façades integrating photovoltaic (PV) panels [77].

The effects of the radiation can be significant on the thermal properties of building facades with ventilated air gaps. These effects involve both convection and radiation heat transfer mechanisms [78,79]. Specifically, the thermal resistance of air cavities can change dynamically over time depending on several parameters, including outdoor conditions (temperature and incident solar radiation) and thermo-physical properties of the building envelope system. No experimental testing analyses have been reported on ventilated facades using hot box apparatuses coupled with solar simulators.

Moreover, the effects of aspect ratio for air gaps within building envelope systems have evaluated for different velocity profiles under steady-state conditions [80]. Similarly, the effects in thermal performance of adding reflective surfaces inside air cavities have been tested [81]. Rahiminejad et al. have proposed new indicators to describe the thermal characteristics the air gaps including apparent thermal resistance and effective thermal resistance using energy balance principles applied to a network of thermal resistances [82]. However, these indicators are suitable for steady-state analysis since they do not consider the effects of solar radiation and thermal inertia.

The performance of opaque façades can be affected by moisture heat transfer. Indeed, differential temperatures drive moisture movement through hygroscopic materials as demonstrated by reported testing analyses using guarded hot box apparatus following ISO 8990 to measure-values for wall specimens made of burn clay bricks and reinforced cement concrete [83] as well as for porous walls made of cork [84].

Fig. 4 summarizes the boundary conditions that were used to represent outdoor environment and determine the performance metrics to characterize dynamic thermal performance of non-adaptive opaque façade systems. In all cases, temperature settings in the chambers reflected realistic conditions as recommended by both standards [42,41].

On the other hand, many testing-based studies did not report crucial parameters for assessing the thermal performance of the evaluated specimens including convective and radiative coefficients or surface resistances required for estimating thermal transmittances and overall thermal resistances of the specimens. Moreover, some studies have not reported all the full details of the testing protocols including air velocities within the chambers as well as within façade specimens with air cavities.

The validity criteria of measurements according to ISO 8990 [41] and ASTM C1363 [42] standards were reported in some cases by reporting the range of temperature variation [66,70,83]. In few cases, reported fluctuations were not meet by followed standard [77,80]. Most of reviewed papers demonstrated stability graphically [67–69,73,75] or qualitatively [72,85,86]. However, several testing studies have not reported and documented the validity criteria of measurements as dictated by the standards [74,81,84].

4. Experimental tests used for adaptive opaque façades

Dynamic thermal performance has been tested using laboratory setups for three different types of adaptive opaque facade technologies when excluding those systems that involve outdoor-indoor air exchanges and PCMs. These technologies include removable insulations, movable insulations, and thermodiodes. This section describes the testing procedures used to characterize the thermal performance for the three technologies including their limitations. Specifically, Section 4.1 describes the characterization of removable insulation under a steady regime. Section 4.2 outlines the testing procedure used to determine the dynamic thermal performance for movable insulation systems. Section 4.3 summarizes the different testing procedures considered for the characterization of thermodiodes, both with natural convection mechanisms and phase change fluids. For the last one, a variation of the technology integrating a PV cladding has been also tested.

4.1. Characterization of removable insulation systems

Removable insulation is a patented technology concept as illustrated in Fig. 5 [87]. The system utilizes a series of vertical opaque films that can be rolled, like conventional blinds. This removable insulation system can be integrated within a closed cavity to minimize the convective losses caused by wind suction and pressure difference. Another possible placement of the removal insulation system is between a massive opaque wall and an external closure panel. For this case, when the films are rolled down the thermal transmittance of the opaque façade is reduced when compared to the same configuration without the insulation system. The air cavity between the closure panel and the massive opaque wall is subdivided into several air layers with small thicknesses [i.e., Fig. 5 (right)]. When the films are up, the small thickness air layers are substituted by a wider air gap, and thus, the thermal losses by convection and radiation would be more significant compared with the previous setting of the insulation system [i.e., Fig. 5 (left)].

Pflug et al. have prototyped this removable insulation concept and measured its maximum thermal conductance using a guarded hot plate apparatus [87]. They have measured the steady-state heat transfer by following the testing protocol of ISO 8302:1991 [40] as described in Section 2. For the estimation of the specimen conductance, a modified calculation method for the uncertainty levels is proposed [40]. This method compares the measurements of the removable insulation concept with a benchmark sample having an equivalent insulation level. The performance of the removable insulation prototype has been tested for a specific fixed position when the films are rolled down, but no testing has been carried out when the films are rolled up.

As part of the testing protocol, outer and inner surface temperatures

PERFORMANCE METRICS		BOUNDARY CONDITIONS							
		Sinusoidal signal	Periodic increase of temperature	Temperature transitions & specific setpoints	Static set points	Air velocity reported	Relative humidity reported	Artificial sun included	Convective coefficient reported
MEASURED	Heat Flow through specimen	[70]				[70]			[70]
	Peak heat flux	[74]							[74]
	Surface temperatures								
	Convective air velocity in the cavity								
	Total stored energy	[73]							
	Stored and released latent heat			[75]				[75]	
	Relative Humidity	[84]							[84]
CALCULATED	Thermal conductivity	[73]	[72]		[77]		[72]	[77]	[77]
	Thermal transmittance	[66, 67, 70]	[68]		[77, 83]	[68, 70, 83]		[77]	[70, 77, 83]
	Thermal Resistance	[85]		[69, 86]	[80, 81]	[81]			
	Decrement Factor	[66, 67, 74, 85]							[74]
	Time lag	[67, 74, 85]		[69]					[74]
	Amplitude			[69]					

Fig. 4. Summary of Experimental tests characterizing the dynamic performance of non-adaptive Opaque Façade components.

as well as heat fluxes through the specimen are measured. Based on measured data, the U-value of the specimen is calculated for five different boundary conditions, by adding to measured thermal conductance both exterior and exterior surface thermal resistances estimated by EN 410:2011 [88] as 0.04 m^2 K/W and 0.13 m^2 K/W, respectively. The temperatures of the hot and cold plates have been changed to impose different temperature gradients between inner and outer layers, as well as to obtain different mean surface temperatures, ranging from 10 °C to 29.3 °C. The reasons for performing the tests under these five boundary conditions are not clearly stated. According to the experimental characterizations, the low U-value ranges from 0.35 ± 0.03 W/m^2K to 0.45 ± 0.03 W/m^2K. However, the obtained U-values are higher than the theoretical values and have a stronger temperature dependance. The authors have used ISO 15099 *Thermal performance of windows, doors and shading devices* to estimate the U-values. For the specimen conductance, a modified calculation method to determine the uncertainty levels was proposed [89]. The authors have indicated that the mismatch between measured and calculated data is due to the airtightness level set by ISO 15099, which is not achieved between air cavities for the tested prototype.

For the removable insulation technology, testing has been performed for the low conductivity settings using relatively small-scale prototypes. The reported analysis demonstrated that the use of guard hot plate method is not the most suitable testing apparatus for the characterization of adaptive façade system, and that the convection within the air cavities should not be neglected.

4.2. Characterization of movable insulation

Another type of adaptive opaque facades involves mechanically operated movable insulation systems [90]. These systems modulate heat flows through the facades depending on the position of their insulation layers. A louvered type of movable insulation system, depicted in Fig. 6, has been tested under laboratory conditions to characterize its dynamic thermal performance [90]. The louvered insulation layers can rotate if actuated by mechanical actuators. When the insulation layers are aligned vertically [Fig. 6 (a)], the system acts as a conventional insulation layer with high R-value. In this setting, the convective heat transfer of the air cavities at both sides of the insulation layer, while minimal, increase the insulation level of the façade and is considered for the U-value/R-value estimation. When the layers are rotated at any specific angle $\theta_i \neq 0$ [Fig. 6 (b)], both air cavities are connected, and convective heat transfer becomes dominant resulting in low R-value for the movable insulation system. The maximum heat transfer in the system is achieved when the louvered insulation layers are set to be parallel (i.e., $\theta_i = 90°$).

Dabbagh and Krarti have built a protype of the movable insulation system representing a full-size panel for building envelope façade (Fig. 7). The thermal performance of the dynamic insulation system is measured using ASTM C1363 and ISO 8990 procedures and a hot-box apparatus, which can be used to test complex assemblies without considering their different components as discussed in Section 2. The objective of the experiment is to estimate the R-value of the movable insulation system.

Two heat flux sensors and surface temperature thermocouples have been placed along the center of the tested specimen. In addition, thermocouples are utilized to measure the air temperatures for both hot and cold chambers. The tests have been carried out under steady-state conditions for various positions (i.e., values for the angle θ_i) of the louvered insulation layers. The reported testing has considered only one boundary condition with the hot chamber set at 77.65 °C, whereas the cold chamber maintained at 28.70 °C. For the tested movable insulation prototype, the maximum and minimum R-values are measured to be 2.30 $m^{2\circ}$C/W (i.e., U-value 0.43 W/$m^{2\circ}$C) and 0.38 $m^{2\circ}$C/W (i.e., U-value 2.63 W/$m^{2\circ}$C), respectively. The uncertainty levels for the measured R-values have been determined using an error propagation analysis, which resulted in 0.17 Km^2/W uncertainty.

One of the limitations of the testing analysis carried out for the movable insulation prototype consists of the fact that only one boundary condition has been considered. Whereas homogeneous materials and layers exhibit similar thermal performance for different boundary conditions (i.e., hot and cold temperatures as well as air velocities), complex assemblies with free natural convection, such as the movable insulation systems, may have thermal performance depending on boundary settings since convective heat transfer can be dependent on surface temperatures as well as air temperatures within the cavities.

4.3. Characterization of thermodiodes

Thermodiodes are thermal components that allow heat transfer only in one desired direction and thus blocking heat from flowing in the opposite direction [91]. Likewise, changes in the surrounding temperatures do not cause heat flow in the undesired direction. A thermodiode facade integrates a pipe-loop which contains a working fluid. One of the façade surfaces acts as a heat collector, whereas the other surface releases the stored heat through radiation. There are two different types of heat transfer mechanisms including (i) natural convection, and (ii) phase change of the working fluid. Unlike multifunctional facades integrating heating or cooling devices, thermodiodes can control heat transfer through adjustments of surrounding environmental conditions with no need of additional heat or cooling sources [92].

4.3.1. Thermodiode by natural convection

Chun et al. have built and tested a thermodiode system that can

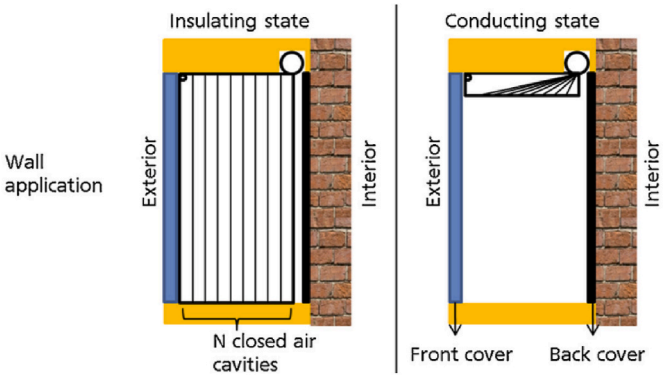

Fig. 5. Removable insulation concept. Source [87].

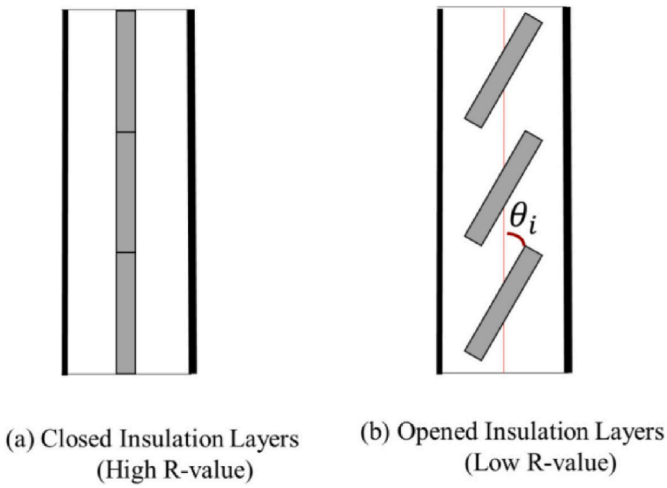

Fig. 6. Movable insulation concept. Source [90].

Fig. 7. Experimental set up for the characterization of Movable Insulation. Source [90].

modify the natural convection direction by mechanically changing the position of its pipes [91]. These pipes have been made of black copper to enhance solar energy absorption. The space between the two plates was filled with glass wool insulation to minimize heat transfer through the façade (Fig. 8). An outer layer of double glass closed the component.

The thermal performance of the thermodiode prototype has been tested for 5 different working fluid types. The specimen has been exposed to a constant air temperature and to synthetic radiation generated by 88 halogen lamps rated at 50 W each during 2- to 4-h periods. Temperatures of various components of the prototype have been measured using thermocouples to estimate heat transfer rates. The reported tests have been performed under steady-state conditions achieved typically 2-h period from the start the experiments. The testing results have indicated similar performance achieved for all the considered working fluids. However, no overall thermal performance for the tested thermodiode protype has been estimated including a U-value or an R-value. This specific technology switches the heat flow direction, but it is unclear if it allows a significant U-value change.

4.3.2. *Thermodiode with phase change fluids*

Tan e Zhang have modelled, built, and tested a wall integrating pipes to transfer collected solar energy to the indoor environment. For this technology, heat transfer is unidirectional and depends on the surface that has the higher temperature [93]. The fluid inside the pipes (i.e., the refrigerant) absorbs solar radiation, evaporates, and then condenses along the inner section, as illustrated by Fig. 9. During cooling mode, when outdoor surface temperatures are lower than the indoor air temperatures, the fluid enhances heat dissipation. With the integration of intelligent control valves, unwanted heat flows can be avoided [94].

The guidelines set by the standard GB/T13475-2008 [94] have been followed to determine steady-state thermal transmission through the tested thermodiode prototype using a calibrated Guard Hot-Box apparatus. This standard is based on ISO 8990, which has been described in Section 2. The maximum U-value of the thermodiode prototype has been measured for different boundary conditions. For the testing protocol, the hot box temperature has been set at 18 °C. The cold box temperatures have been set to reach in the surface of the specimen a calculated solar-air temperature range of a typical day. The heating power of the cold box is adjusted to reach an expected incremental increase of 2 °C from 24 °C to 40 °C in the outer surface. According to the tests' results, for the tested boundary conditions U-value increases with outside surface temperatures, varying between 0.77 W/m^{2}K and 1.05 W/m^{2}K. No tests have been performed for the case with minimized heat transfer when the inside surface temperature is higher than that of the outside surface of the evaluated façade.

More recently, the same technology has been tested using a hot box apparatus to determine its time lag, decrement factor, response time, and operating time [95] (Fig. 10). First, a steady state evaluation of a reference wall integrating heat pipes is carried out, but without

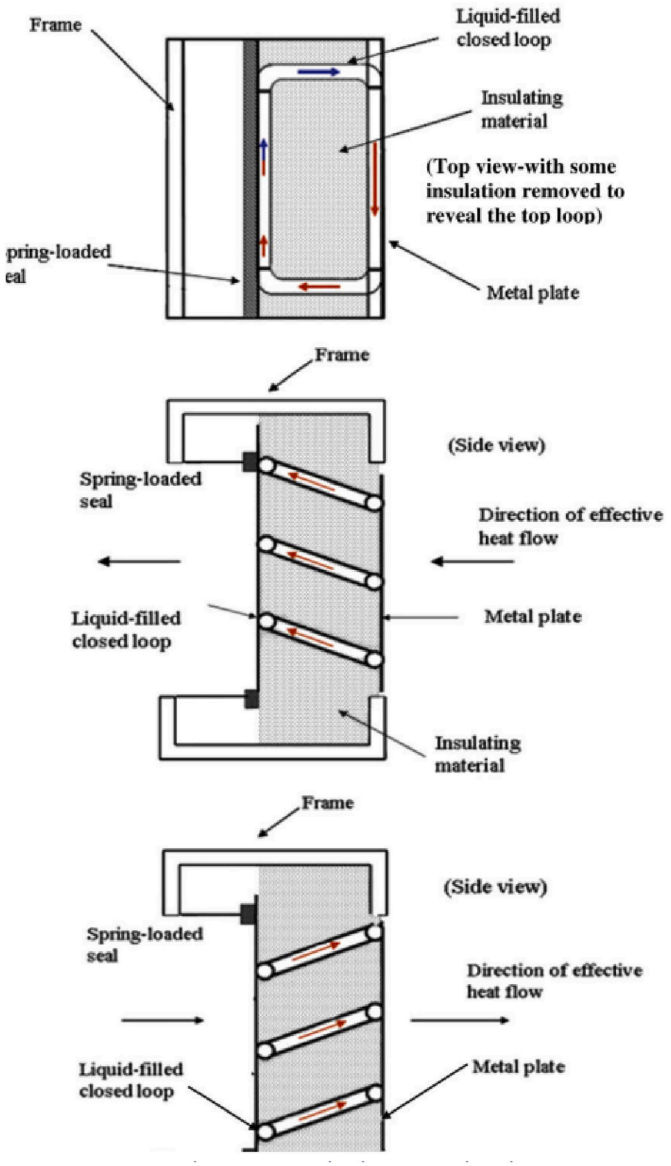

Fig. 8. Bi-directional thermodiode concept. Source [91].

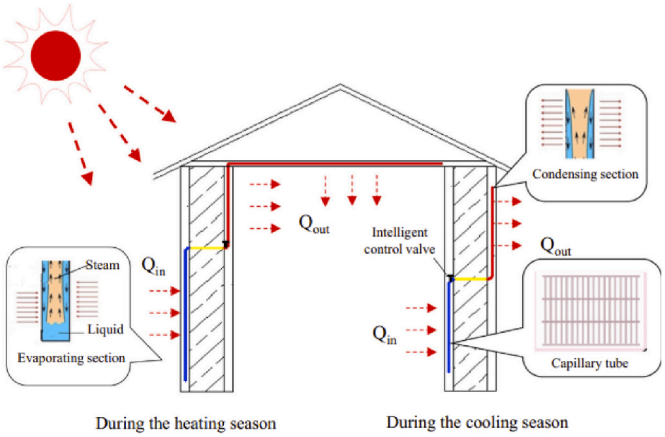

Fig. 9. Unidirectional diode with phase change fluids concept. Source [93].

including any phase change fluid. For this reference wall, surface temperatures have been measured to estimate the time lag and the decrement factor. Only the temperature of the hot box chamber has been controlled to maintain a constant temperature of 40 °C. The cold chamber with its door kept open has its temperature to be the same as the air temperature of the laboratory. Then, the effects of the fluid phase change have been evaluated for the same boundary conditions using eighteen surface temperature sensors placed on both surfaces. The thermal performance of the wall integrating the pipes has been compared to that achieved by the reference wall using Temperature Rise Coefficient (β), which expresses the change of the temperature of the pipe's section (Tc) relative to the temperature of the of the reference wall ($T_{s,a}$), normalized by the difference between the solar air temperature (T_z) and inside surface temperature ($T_{s,b}$) as expressed by Equation (7):

$$\beta = \frac{T_c - T_{s,a}}{T_z - T_{s,b}} \tag{7}$$

A maximum Temperature Rise Coefficient of 0.11 has been estimated based on the testing analysis. The response time of the adaptive opaque façade system has been also estimated when the fluid starts to evaporate within the pipes. For steady state testing analysis, the response time has been measured to be 40 min. For dynamic testing analysis, solar air temperature variation for a typical day has been set for the hot box chamber, with minimum and maximum temperatures of 7 °C and 35.5 °C, respectively. The Temperature Rise Coefficient and response time values estimated using dynamic testing conditions are determined to be 0.39 and 20 min, respectively. The thermal characterization of the tested system includes its heat transfer capacity, calculated using the heat transfer coefficient, temperature difference, and area of the specimen. For the reference wall, the maximum heat transfer capacity value is determined to be 3.17 W/m^2, whereas it is 9.93 W/m^2 for the wall integrating pipes. These results demonstrated that the technology efficiently transfers heat, with a faster response to environmental conditions than the reference wall.

The used tests effectively have captured the benefits of having a phase change fluid integrated in a thermodiode measuring several key performance metrics. However, the reported testing analysis has not been used to estimate the equivalent U-value/R-value range, hampering a direct comparison of the thermal performance of the evaluated prototype with other opaque facades including both dynamic and static systems.

Pugsley et al. have characterized through experimental testing two variants of thermodiodes with phase change fluids [96]. Pugsley et al. built and tested first a thermodiode equipped with evaporator and condenser plates separated by a cavity as shown in Fig. 11.

Specific testing set-up has been developed and applied to estimate an equivalent U-value for both heat flux directions. This set up controls the temperature difference between the evaporator and condenser plates by connecting them separately to a heating–cooling fluid circuit to maintain through automatic control the desired set temperature. Fluid flows and return temperatures have been measured to quantify heat losses.

The measured parameters have included surface temperatures, fluid rates, and pressures. The energy consumed by the heating-cooling circuit has been also measured. The tests have been performed under different surface temperatures for the evaporative plate. For all the tests, a temperature gradient of 20 °C between the inner and outer plates (i.e., evaporator and condenser plates) has been set to assess the temperature variations experienced by the working fluid. The maximum U-values have been achieved when surface temperatures are the highest and are measured to be 12 W/m^{2}K for the thermal flux flowing from inner to outer surfaces and 1200 W/m^{2}K for the other flux direction. The U-values of reverse direction (i.e., from inside to outside) have increased slightly incrementally when the fluid temperatures are increased.

The measurement uncertainty levels for the tests have been reported to be 25%. These high uncertainties have been attributed to the small temperature differences and possibly inaccurate estimations of fluid convection heat transfers. To achieve more accurate measurements, the authors suggested testing using a hot-box apparatus. The U-values of the prototype have not been reported when the control valves are close.

The second set of tests performed by Pugsley et al. has considered a thermodiode prototype integrating photovoltaic cells placed on its transparent acrylic external cladding (Fig. 12).

The tests of the PV-integrated thermodiode prototype have been performed under various dynamic conditions using different solar irradiances on the vertical plane. The tests include daytime solar heat collection of 6-h periods and a cool overnight of 18-h periods. During the daytime periods, the heat flux direction is from the outside cladding to the inside, whereas during the night periods, heat flow is reversed from inside to the outside.

The testing set up consists of an artificial light source placed in a room with a controllable air temperature. As done for testing the first thermodiode prototype, temperatures of different components, flow rates, and pressures have been measured to estimate equivalent U-values for both heat flow directions. The energy consumed by the heating/cooling loop has been also measured. A total of 50 thermocouples have been installed to perform the testing analysis Using different light source setting (G = 870, 610 and 370 W m^2). A calibrated pyranometer have been used to check the radiation uniformity over the whole surface area to be within± 10%.

During testing cases when the façade has been exposed to solar radiation, a maximum equivalent U-value of 900 W/m^{2}K has been

Fig. 10. Hot box apparatus used for the characterization of a Unidirectional Thermodiode with phase change. Source [95].

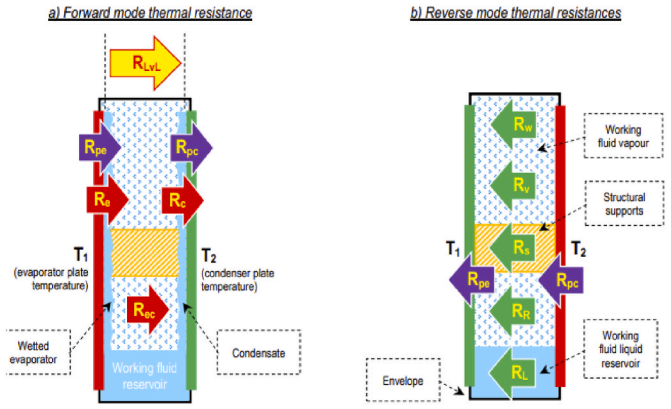

Fig. 11. One of the technology concept characterized by Pugsley et al. Source [96].

measured for high temperatures. This U-value is decreased to only 50 W/m^{2}K when the specimen has been exposed to low temperatures. For tests carried out during periods with no solar irradiance, the equivalent U-value has been estimated to range between 1.6 and 1.9 W/m^{2}K, slightly increasing with temperature.

One of the biggest issues of the testing analysis of the thermodiode prototypes includes the lack of uniformity of the evaporating wetting as identified using thermographic camera. No uncertainty analysis of the experimental results has been carried out for the second set of experiments specific to the PV-integrated thermodiode prototype.

4.4. Comparison of the different testing approaches: identifying the successes, limitations and omissions

The characterization of thermal performance of adaptive opaque façade systems have been reported using various testing set-ups and protocols as summarized in Table 5. Hot box apparatuses are generally the most used testing set-up.

Almost all reported adaptive building envelope systems have been tested under various steady-state and some dynamic environmental conditions Fig. 13. However, none of the tests provided a full characterization of the adaptive thermal performance. For instance, testing analyses reporting maximum U-values have not quantified the minimum U-values for the evaluated adaptive facades. The characterization of the thermal flux in both directions have been only carried out for some thermodiode cases. Some studies have suggested new performance metrics such as the temperature rise coefficient, proposed by Ref. [95], to highlight the difference in thermal performance between static and adaptive façades. However, this performance metrics should be coupled with other metrics to make fair comparison between static and adaptive facades. Some of these other thermal performance metrics measured through the reported studies include decrement factors and time lags. All the reported testing analyses do not evaluate the dynamic thermal performance adaptive facades when they transition from different heat transfer modes (i.e., from low to high R-value settings). Indeed, all the reported tests have been performed having the adaptive facades set in specific "static" positions. Thus, any features related to the transition phases of the adaptive facades have not been measured and reported including the time needed to reach any specific setting and the energy input required to shift from one state to another [14].

As noted for testing the thermal performance of static opaque façade systems outlined in Section 3, none of the reported experimental analyses for adaptive building envelope prototypes have indicated the specific air-velocities of the used hot-box set ups. As explained in Section 2, the boundary conditions including air velocities can have significant effects on the overall thermal performance of adaptive facades. For testing any static and adaptive façade system using hot box apparatus, it is good practice to fully characterize all the boundary conditions through the use of sufficient sensors within both chambers of the hot box set-up as well as components of the evaluated specimen including façade surfaces especially for those systems made-up of multiple layers and air cavities.

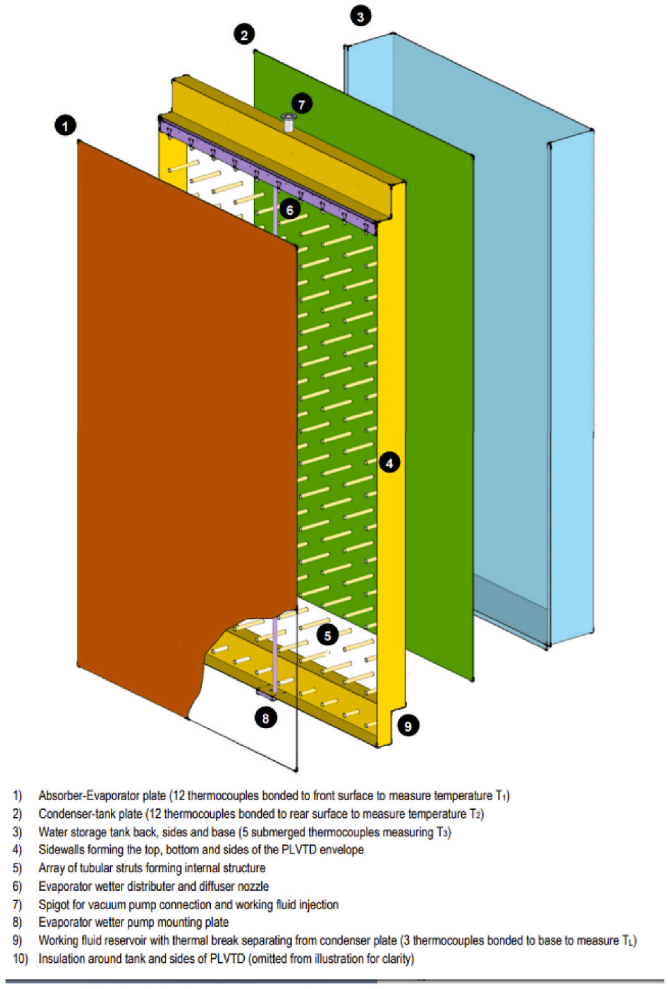

Fig. 12. Technology concept of the thermodiode integrating photovoltaic cells. Source [96].

5. Summary and conclusions

This paper reviewed the experimental testing protocols specific to adaptive opaque façade systems that have dynamic heat transmission characteristics without any air-flow exchanges between indoors and outdoors. The results of the experimental testing are valuable to validate analytical and/or simulation models for the adaptive facades. It is found that the reported testing approaches have substantial differences in both the set-up configurations and the testing protocols. Based on these findings, the following suggestions can be made to ensure a more complete testing procedure to characterize the dynamic thermal performance of opaque façade components.

5.1. Performance metrics: measurements & calculations

- The complexity of heat transfer specific to adaptive opaque façades can be overcome by considering their thermal performance holistically, without characterizing the thermal response of each element. Equivalent Thermal Transmittance (U-value) or Resistance (R-value) are suitable metrics, which can be estimated by measuring the inner and outer surface temperatures and heat-fluxes. These metrics can then be readily compared with the U-values and R-values of conventional opaque façade systems.
- Adaptive opaque façade systems can modulate their thermal performance (i.e., U-value) using various adaptation mechanisms and ranges. Therefore, any testing protocol should provide at least the maximum and minimum equivalent U-values for the different configurations of the adaptive façades, under the same boundary conditions.
- The characteristics of some adaptive opaque facades can depend on the direction of the heat flux such is the case of thermodiodes. Thus, the maximum equivalent U-values of these facades should be measured for both heat transfer directions.
- The adaptation velocity or the switching velocity is a key parameter that characterizes the thermal performance of adaptive façades. Most of the reported testing studies have indicated the time required to reach steady-state conditions when transitioning from one boundary conditions to another. However, the adaptation velocity for adaptive facades refers to the time needed to change from low to high U-

Table 5
Set ups and protocols used for the thermal characterization of adaptive opaque facade systems.

		Followed standard				
		ISO 8302:1991	ASTM C1363	ISO 8990	GB/T13475-2008 (based on ISO 8990)	None
Set up	**Hot-box apparatus**		Movable Insulation [90]	Movable Insulation [90]	Uni-directional thermodiode by phase change [95]	
	Guarded hot plate apparatus	Removable insulation [87]			Uni-directional thermodiode by phase change [93]	
	Set-up including solar simulator					Bi-directional thermodiode by natural convection [91] Uni-directional thermodiode by phase change with and without PV [96]

PERFORMANCE METRIC		BOUNDARY CONDITIONS				
		Performance metrics for all the adaptive stages	Velocity of adaptation	Thermal flux in both directions	Steady state	Dynamic
MEASURED	Heat flux	[90]	[95]		[87, 90, 95]	[93, 95]
	Surface Temperature	[90]	[95]		[90, 91, 95, 96]	[93, 95, 96]
	Fluid rate				[96]	
	Pressure				[96]	
	Fluid temperature					[96]
CALCULATED	U or R value	[90]		[96]	[87, 90, 96]	[93, 96]
	Heat transfer rate of the working fluid				[91]	
	Time lag		[95]		[95]	[95]
	Decrement factor		[95]			[95]

Fig. 13. Summary of the thermal characterization tests of adaptive opaque façade systems: relationship between the performance metrics and testing boundary conditions.

values and vice-versa. Therefore, specific tests should be carried out for adaptive opaque facades to measure the time that it takes to reach steady-state conditions once their switching mechanism is triggered. The tests should determine if this time is the same when switching from low to high U-values and from high to low U-values.

- Apart from the laboratory testing, to properly characterize the performance of adaptive facades, it is necessary to quantify the energy demand required by the actuators triggering the switching of their thermal properties, as well as the durability (adaptation cycles) of these actuators.

5.2. Boundary conditions of experimental tests

- The equivalent U-values or R-values of the opaque facades include radiative and convective effects along the surfaces. If simplified coefficients are used to define external and internal surface resistances, then it is essential to ensure that the boundary conditions that are being applied for the testing protocols match those used in estimating these coefficients. Thus, it is a good practice to report the boundary conditions of the tests, including air velocities within the chambers, for better understanding of the results and for the replicability of the experiments.
- When naturally induced convective heat transfer play an important role in modulating the thermal performance of adaptive opaque façades, the temperature of the fluid could influence their equivalent U-values. The boundary conditions used in the testing protocols should be realistic, so that the fluid inducing the convective heat transfer reaches reasonable temperatures. It is recommended that different extreme realistic boundary conditions should be tested to assess if the equivalent U-values change substantially with the environmental conditions. Tests under dynamic conditions give valuable insights on the heat storage capabilities and the thermal inertia of adaptive opaque facades especially those integrating phase change materials and/or fluids. The challenge of these dynamic tests is to measure the equivalent U-values, time lags, decrement factors and response times for different dynamic periods. It is important to consider dynamic tests using realistic boundary conditions for representative typical summer/winter/midseason weeks. Another alternative approach discussed in this review is to vary the outdoor temperature using a sinusoidal function with time. By performing tests for these dynamic boundary conditions, the dynamic heat transfer and the thermal storage properties of the adaptive facades can be measured.

5.3. Testing protocols & validity criteria

- The number of the sensors and their placement should be determined to consider any heterogeneity of the adaptive façade assemblies. In

particular, sensors should cover any façade's discontinuities, such as those associated with the presence of embedded pipes or air cavities, so an average or an equivalent U-value/R-value can be estimated accurately.

- It is essential that the tested specimen be air-tight to ensure that there is no air-flow exchange between the two chambers representing the indoors and outdoors. Otherwise, it may not be possible to accurately measure the equivalent U-values of these tested specimen by following ISO 8990 and ASTM C1363 standards.
- It is crucial to estimate the uncertainty levels of the measured thermal properties of the tested adaptive opaque facades. The measurements should be carried out using the stability conditions defined in ISO 8990 or ASTM C1363 standards.

5.4. Future research

Future research needs to perform dynamic thermal performance characterizations of adaptive opaque façade systems by following these recommendations, to better measure their specific properties under realistic operation conditions. Overall, more experimental characterizations are needed to increase the technology readiness of adaptive opaque facades, to bring them closer to their market adoption by the building industry.

CRediT authorship contribution statement

Miren Juaristi: Writing – original draft, Investigation, Data curation, Conceptualization. **Moncef Krarti:** Writing – review & editing, Supervision, Methodology, Conceptualization.

Declaration of competing interest

The authors declare the following financial interests/personal relationships which may be considered as potential competing interests: Miren Juaristi reports travel was provided by Autonomous Province of Bolzano - South Tyrol.

Data availability

In this review the data comes from the papers that were cited as reference.

Acknowledgments

This paper has been funded by the Autonomous Province of Bolzano/Bozen South Tyrol, Italy, in the framework of the Programme "Short international research stays".

References

[1] L.F. Cabeza, M. Chàfer, Technological options and strategies towards zero energy buildings contributing to climate change mitigation: a systematic review, Energy Build. 219 (2020) 9, https://doi.org/10.1016/j.enbuild.2020.110.
[2] L. Belussi, et al., A review of performance of zero energy buildings and energy efficiency solutions, in: Journal of Building Engineering, vol. 25, Elsevier Ltd, 2019, https://doi.org/10.1016/j.jobe.2019.100772.
[3] W.A. Friess, K. Rakhshan, M.P. Davis, A global survey of adverse energetic effects of increased wall insulation in office buildings: degree day and climate zone indicators, Energy Effic. 10 (1) (2017) 97–116, https://doi.org/10.1007/s12053-016-9441-z.
[4] K.M.S. Chvatal, H. Corvacho, The impact of increasing the building envelope insulation upon the risk of overheating in summer and an increased energy consumption, J. Build. Perform. Simul. 2 (4) (2009) 267–282, https://doi.org/10.1080/19401490903095865.
[5] Q. Jin, F. Favoino, M. Overend, Design and control optimisation of adaptive insulation systems for office buildings. Part 2: a parametric study for a temperate climate, Energy 127 (2017) 634–649, https://doi.org/10.1016/j.energy.2017.03.096.
[6] COST ACTION TU1403 – Adaptive Facade Network." http://tu1403.eu (accessed Nov. 16, 2017).
[7] R.C.G.M. Loonen, M. Trčka, D. Cóstola, J.L.M. Hensen, Climate adaptive building shells: state-of-the-art and future challenges, Renew. Sustain. Energy Rev. 25 (2013) 483–493, https://doi.org/10.1016/j.rser.2013.04.016.
[8] A. Zuazua-Ros, C. Martín-Gómez, E. Ibañez-Puy, M. Vidaurre-Arbizu, Y. Gelbstein, Investigation of the thermoelectric potential for heating, cooling and ventilation in buildings: characterization options and applications, in: Renewable Energy, vol. 131, Elsevier Ltd, 2019, pp. 229–239, https://doi.org/10.1016/j.renene.2018.07.027.
[9] A. Prieto, U. Knaack, T. Auer, T. Klein, COOLFACADE: state-of-the-art review and evaluation of solar cooling technologies on their potential for façade integration, in: Renewable and Sustainable Energy Reviews, vol. 101, Elsevier Ltd, 2019, pp. 395–414, https://doi.org/10.1016/j.rser.2018.11.015.
[10] Y. Luo, L. Zhang, M. Bozlar, Z. Liu, H. Guo, F. Meggers, Active building envelope systems toward renewable and sustainable energy, in: Renewable and Sustainable Energy Reviews, vol. 104, Elsevier Ltd, 2019, pp. 470–491, https://doi.org/10.1016/j.rser.2019.01.005.
[11] M. Juaristi, T. Gómez-Acebo, A. Monge-Barrio, Qualitative analysis of promising materials and technologies for the design and evaluation of Climate Adaptive Opaque Façades, Build. Environ. 144 (2018) 482–501, https://doi.org/10.1016/j.buildenv.2018.08.028.
[12] H. Cui, M. Overend, A review of heat transfer characteristics of switchable insulation technologies for thermally adaptive building envelopes, Energy Build. 199 (2019) 427–444, https://doi.org/10.1016/j.enbuild.2019.07.004.
[13] Y. Yang, S. Chen, Thermal insulation solutions for opaque envelope of low-energy buildings: a systematic review of methods and applications, in: Renewable and Sustainable Energy Reviews, vol. 167, Elsevier Ltd, 2022, https://doi.org/10.1016/j.rser.2022.112738.
[14] A. Karanafti, T. Theodosiou, K. Tsikaloudaki, Assessment of buildings' dynamic thermal insulation technologies-A review, in: Applied Energy, vol. 326, Elsevier Ltd, 2022, https://doi.org/10.1016/j.apenergy.2022.119985.
[15] M. Fawaier, B. Bokor, Dynamic insulation systems of building envelopes: a review, in: Energy and Buildings, vol. 270, Elsevier Ltd, 2022, https://doi.org/10.1016/j.enbuild.2022.112268.
[16] A. Shafaghat, A. Keyvanfar, Dynamic façades design typologies, technologies, measurement techniques, and physical performances across thermal, optical, ventilation, and electricity generation outlooks, in: Renewable and Sustainable Energy Reviews, vol. 167, Elsevier Ltd, 2022, https://doi.org/10.1016/j.rser.2022.112647.
[17] K. Martin-Escudero, E. Salazar-Herran, A. Campos-Celador, G. Diarce-Belloso, I. Gomez-Arriaran, Solar energy system for heating and domestic hot water supply by means of a heat pump coupled to a photovoltaic ventilated façade, Sol. Energy 183 (2019) 453–462, https://doi.org/10.1016/j.solener.2019.03.058.
[18] D. Wang, et al., Classification, experimental assessment, modeling methods and evaluation metrics of Trombe walls, in: Renewable and Sustainable Energy Reviews, vol. 124, Elsevier Ltd, 2020, https://doi.org/10.1016/j.rser.2020.109772.
[19] C. Lamnatou, G. Notton, D. Chemisana, C. Cristofari, Storage systems for building-integrated photovoltaic (BIPV) and building-integrated photovoltaic/thermal (BIPVT) installations: environmental profile and other aspects, in: Science of the Total Environment, vol. 699, Elsevier B.V., 2020, https://doi.org/10.1016/j.scitotenv.2019.134269.
[20] A.A.M. Omara, A.A.A. Abuelnuor, Trombe walls with phase change materials: a review, Energy Stor. 2 (6) (2020), https://doi.org/10.1002/est2.123.
[21] Q. Xiong, et al., Application of phase change material in improving trombe wall efficiency: an up-to-date and comprehensive overview, in: Energy and Buildings, vol. 258, Elsevier Ltd, 2022, https://doi.org/10.1016/j.enbuild.2021.111824.
[22] K. Sergei, C. Shen, Y. Jiang, A review of the current work potential of a trombe wall, in: Renewable and Sustainable Energy Reviews, vol. 130, Elsevier Ltd, 2020, https://doi.org/10.1016/j.rser.2020.109947.
[23] A.A. Abed, O.K. Ahmed, M.M. Weis, K.I. Hamada, Performance augmentation of a PV/Trombe wall using Al2O3/Water nano-fluid: an experimental investigation, Renew. Energy 157 (2020) 515–529, https://doi.org/10.1016/j.renene.2020.05.052.
[24] J. Böke, U. Knaack, M. Hemmerling, State-of-the-art of intelligent building envelopes in the context of intelligent technical systems, in: Intelligent Buildings International, vol. 11, Taylor and Francis Ltd., 2019, pp. 27–45, https://doi.org/10.1080/17508975.2018.1447437, no. 1.
[25] S. Attia, S. Bilir, T. Safy, C. Struck, R. Loonen, F. Goia, Current trends and future challenges in the performance assessment of adaptive façade systems, Energy Build. 179 (2018) 165–182, https://doi.org/10.1016/j.enbuild.2018.09.017.
[26] B. Park, W.v. Srubar, M. Krarti, Energy performance analysis of variable thermal resistance envelopes in residential buildings, Energy Build. 103 (2015) 317–325, https://doi.org/10.1016/j.enbuild.2015.06.061.
[27] K. Menyhart, M. Krarti, Potential energy savings from deployment of Dynamic Insulation Materials for US residential buildings, Build. Environ. 114 (2017) 203–218, https://doi.org/10.1016/j.buildenv.2016.12.009.
[28] S. Rupp, M. Krarti, Analysis of multi-step control strategies for dynamic insulation systems, Energy Build. 204 (2019), https://doi.org/10.1016/j.enbuild.2019.109459.
[29] A.H.A. Dehwah, M. Krarti, Cost-benefit analysis of retrofitting attic-integrated switchable insulation systems of existing US residential buildings, Energy 221 (2021), https://doi.org/10.1016/j.energy.2021.119840.
[30] A.H.A. Dehwah, M. Krarti, Optimal controls of precooling strategies using switchable insulation systems for commercial buildings, Appl. Energy 320 (2022), https://doi.org/10.1016/j.apenergy.2022.119298.

[31] B. Park, M. Krarti, Energy performance analysis of variable reflectivity envelope systems for commercial buildings, Energy Build. 124 (2016) 88–98, https://doi.org/10.1016/j.enbuild.2016.04.070.
[32] F. Favoino, Q. Jin, M. Overend, Design and control optimisation of adaptive insulation systems for office buildings. Part 1: adaptive technologies and simulation framework, Energy 127 (March) (2017) 301–309, https://doi.org/10.1016/j.energy.2017.03.083.
[33] M Juaristi, F Favoino, T Gómez-Acebo, A Monge-Barrio, Adaptive opaque façades and their potential to reduce thermal energy use in residential buildings: A simulation-based evaluation, J. Build. Phys. 45 (5) (2022) 675–720, https://doi.org/10.1177/17442591211045418.
[34] G. Zhou, M. Pang, Experimental investigations on the performance of a collector-storage wall system using phase change materials, Energy Convers. Manag. 105 (2015) 178–188, https://doi.org/10.1016/j.enconman.2015.07.070.
[35] Z. Liu, et al., A review on macro-encapsulated phase change material for building envelope applications, in: Building and Environment, vol. 144, Elsevier Ltd, 2018, pp. 281–294, https://doi.org/10.1016/j.buildenv.2018.08.030.
[36] Q. Al-Yasiri, M. Szabó, Incorporation of phase change materials into building envelope for thermal comfort and energy saving: a comprehensive analysis, in: Journal of Building Engineering, vol. 36, Elsevier Ltd, 2021, https://doi.org/10.1016/j.jobe.2020.102122.
[37] N. Soares, C. Martins, M. Gonçalves, P. Santos, L.S. da Silva, J.J. Costa, Laboratory and in-situ non-destructive methods to evaluate the thermal transmittance and behavior of walls, windows, and construction elements with innovative materials: a review, in: Energy and Buildings, vol. 182, Elsevier Ltd, 2019, pp. 88–110, https://doi.org/10.1016/j.enbuild.2018.10.021.
[38] ISO 9869-1, Thermal Insulation, Building Elements, In-Situ Measurement of Thermal Resistance and Thermal Transmittance-Part 1: Heat Flow Meter Method, 2014.
[39] ISO 8301, Thermal Insulation-Determination of Steady-State Thermal Resistance and Related Properties-Heat Flow Meter Apparatus, 1991.
[40] ISO 8302, Thermal Insulation– Determination of Steady-State Thermal Resistance and Related Properties–Guarded Hot Plate Apparatus, 1991.
[41] ISO 8990, Thermal Insulation - Determination of Steady-State Thermal Transmission Properties - Calibrated and Guarded Hot Box, 1994.
[42] ASTM C1363-19, Standard Test Method for Thermal Performance of Building Materials and Envelope Assemblies by Means of a Hot Box Apparatus, 2021.
[43] B.S. Institution, Thermal Performance of Buildings: Qualitative Detection of Thermal Irregularities in Building Envelopes: Infrared Method (ISO 6781: 1983 Modified), British Standards Institution, 1999.
[44] ISO 10878, Non-destructive Testing–Infrared Thermography: Vocabulary, 2013.
[45] ISO 9869-2, Thermal Insulation — Building Elements — In-Situ Measurement of Thermal Resistance and Thermal Transmittance — Part 2: Infrared Method for Frame Structure Dwelling, 2018.
[46] I. Nardi, E. Lucchi, T. de Rubeis, D. Ambrosini, Quantification of heat energy losses through the building envelope: a state-of-the-art analysis with critical and comprehensive review on infrared thermography, in: Building and Environment, vol. 146, Elsevier Ltd, 2018, pp. 190–205, https://doi.org/10.1016/j.buildenv.2018.09.050.
[47] T. de Rubeis, M. Muttillo, I. Nardi, L. Pantoli, V. Stornelli, D. Ambrosini, Integrated measuring and control system for thermal analysis of buildings components in hot box experiments, Energies 12 (11) (2019), https://doi.org/10.3390/en12112053.
[48] T. de Rubeis, L. Evangelisti, C. Guattari, P. de Berardinis, F. Asdrubali, D. Ambrosini, On the influence of environmental boundary conditions on surface thermal resistance of walls: experimental evaluation through a Guarded Hot Box, Case Stud. Therm. Eng. 34 (2022), https://doi.org/10.1016/j.csite.2022.101915.
[49] M. Andreotti, M. Calzolari, P. Davoli, L.D. Pereira, E. Lucchi, R. Malaguti, Design and construction of a new metering hot box for the in situ hygrothermal measurement in dynamic conditions of historic masonries, Energies 13 (11) (2020), https://doi.org/10.3390/en13112950.
[50] A. Alongi, A. Angelotti, L. Mazzarella, Analytical modelling of breathing walls: experimental verification by means of the dual air vented thermal box lab facility, in: Energy Procedia, Elsevier Ltd, 2017, pp. 36–47, https://doi.org/10.1016/j.egypro.2017.11.121.
[51] D. Sukamto, M. Siroux, F. Gloriant, Hot box investigations of a ventilated bioclimatic wall for NZEB building Façade, Energies 14 (5) (2021), https://doi.org/10.3390/en14051327.
[52] A. J. H. Frijns and L. A. Van Schaijk, "Transparent Dynamic Insulation: a Novel System Combining Ventilation and Insulation for Sustainable Greenhouse Applications", doi: 10.34641/clima.2022.416..
[53] R. Li, X. Wei, H. Li, J. Zhu, Experimental study on ventilation and thermal performance of exterior sandwich wall based on hot box method, in: Procedia Engineering, Elsevier Ltd, 2017, pp. 2771–2778, https://doi.org/10.1016/j.proeng.2017.09.876.
[54] E. Lucchi, F. Roberti, T. Alexandra, Definition of an experimental procedure with the hot box method for the thermal performance evaluation of inhomogeneous walls, Energy Build. 179 (2018) 99–111, https://doi.org/10.1016/j.enbuild.2018.08.049.
[55] M. Madrid, A. Orbe, H. Carré, Y. García, Thermal performance of sawdust and lime-mud concrete masonry units, Construct. Build. Mater. 169 (2018) 113–123, https://doi.org/10.1016/j.conbuildmat.2018.02.193.
[56] P. Santos, M. Gonçalves, C. Martins, N. Soares, J.J. Costa, Thermal transmittance of lightweight steel framed walls: experimental versus numerical and analytical approaches, J. Build. Eng. 25 (2019), 100776, https://doi.org/10.1016/j.jobe.2019.100776.
[57] J.S. Wang, C. Demartino, Y. Xiao, Y.Y. Li, Thermal insulation performance of bamboo- and wood-based shear walls in light-frame buildings, Energy Build. 168 (2018) 167–179, https://doi.org/10.1016/j.enbuild.2018.03.017.
[58] A. Levinskytė, R. Bliūdžius, A. Burlingis, and T. Makaveckas, "Dependencies of heat transmittance through the ventilated wall system on thermal conductivity of connectors crossing thermal insulation layer", doi: 10.1051/matecconf/201928..
[59] A. Ghosh, A. Ghosh, S. Neogi, Reuse of fly ash and bottom ash in mortars with improved thermal conductivity performance for buildings, Heliyon 4 (2018) 934, https://doi.org/10.1016/j.heliyon.2018.
[60] T. de Rubeis, 3D-Printed blocks: thermal performance analysis and opportunities for insulating materials, Sustainability 14 (3) (2022), https://doi.org/10.3390/su14031077.
[61] K. Biswas, A. Desjarlais, D. Smith, J. Letts, J. Yao, T. Jiang, Development and thermal performance verification of composite insulation boards containing foam-encapsulated vacuum insulation panels, Appl. Energy 228 (2018) 1159–1172, https://doi.org/10.1016/j.apenergy.2018.06.136.
[62] C. Buratti, E. Belloni, E. Lascaro, F. Merli, P. Ricciardi, Rice husk panels for building applications: thermal, acoustic and environmental characterization and comparison with other innovative recycled waste materials, Construct. Build. Mater. 171 (2018) 338–349, https://doi.org/10.1016/j.conbuildmat.2018.03.089.
[63] B. Seng, C. Magniont, S. Lorente, Characterization of a precast hemp concrete. Part I: physical and thermal properties, J. Build. Eng. 24 (2019), https://doi.org/10.1016/j.jobe.2018.07.016.
[64] S. Verbeke, A. Audenaert, Thermal inertia in buildings: a review of impacts across climate and building use, Renew. Sustain. Energy Rev. 82 (2018) 2300–2318, https://doi.org/10.1016/j.rser.2017.08.083.
[65] K. Ulgen, Experimental and theoretical investigation of effects of wall's thermophysical properties on time lag and decrement factor, Energy Build. 34 (2002) 273–278.
[66] E. Gengembre, K. Jacquemet, Static and dynamic thermal characterization of facade with mineral foam insulation using a hot-box apparatus, in: Journal of Physics: Conference Series, IOP Publishing Ltd, 2021, https://doi.org/10.1088/1742-6596/2069/1/012089.
[67] Z. Shen, A.L. Brooks, Y. He, S.S. Shrestha, H. Zhou, Evaluating dynamic thermal performance of building envelope components using small-scale calibrated hot box tests, Energy Build. 251 (2021), https://doi.org/10.1016/j.enbuild.2021.111342.
[68] K. Martín, I. Flores, C. Escudero, A. Apaolaza, J.M. Sala, Methodology for the calculation of response factors through experimental tests and validation with simulation, Energy Build. 42 (4) (2010) 461–467, https://doi.org/10.1016/j.enbuild.2009.10.015.
[69] G. Baldinelli, F. Bianchi, A.A. Lechowska, J.A. Schnotale, Dynamic thermal properties of building components: hot box experimental assessment under different solicitations, Energy Build. 168 (2018) 1–8, https://doi.org/10.1016/j.enbuild.2018.03.001.
[70] K. Trgala, M. Pavelek, R. Wimmer, Energy performance of five different building envelope structures using a modified Guarded Hot Box apparatus—comparative analysis, Energy Build. 195 (2019) 116–125, https://doi.org/10.1016/j.enbuild.2019.04.036.
[71] C.A. Ikutegbe, M.M. Farid, Application of phase change material foam composites in the built environment: a critical review, in: Renewable and Sustainable Energy Reviews, vol. 131, Elsevier Ltd, 2020, https://doi.org/10.1016/j.rser.2020.110008.
[72] C. Amaral, R. Vicente, V.M. Ferreira, T. Silva, Polyurethane foams with microencapsulated phase change material: comparative analysis of thermal conductivity characterization approaches, Energy Build. 153 (2017) 392–402, https://doi.org/10.1016/j.enbuild.2017.08.019.
[73] M. Bahrar, Z.I. Djamai, M. el Mankibi, A. Si Larbi, M. Salvia, Numerical and experimental study on the use of microencapsulated phase change materials (PCMs) in textile reinforced concrete panels for energy storage, Sustain. Cities Soc. 41 (2018) 455–468, https://doi.org/10.1016/j.scs.2018.06.014.
[74] Y. Gao, et al., Thermal behavior analysis of hollow bricks filled with phase-change material (PCM), J. Build. Eng. 31 (2020), https://doi.org/10.1016/j.jobe.2020.101447.
[75] Y. Hu, P.K. Heiselberg, H. Johra, R. Guo, Experimental and numerical study of a PCM solar air heat exchanger and its ventilation preheating effectiveness, Renew. Energy 145 (2020) 106–115, https://doi.org/10.1016/j.renene.2019.05.115.
[76] F. Chen, S.K. Wittkopf, P. Khai Ng, H. Du, Solar heat gain coefficient measurement of semi-transparent photovoltaic modules with indoor calorimetric hot box and solar simulator, Energy Build. 53 (2012) 74–84, https://doi.org/10.1016/j.enbuild.2012.06.005.
[77] A. Radwan, T. Katsura, S. Memon, A.A. Serageldin, M. Nakamura, K. Nagano, Thermal and electrical performances of semi-transparent photovoltaic glazing integrated with translucent vacuum insulation panel and vacuum glazing, Energy Convers. Manag. 215 (2020), https://doi.org/10.1016/j.enconman.2020.112920.
[78] M. Rahiminejad, D. Khovalyg, Review on ventilation rates in the ventilated air-spaces behind common wall assemblies with external cladding, Build. Environ. 190 (2021), 107538, https://doi.org/10.1016/j.buildenv.2020.107538.
[79] M. Rahiminejad, D. Khovalyg, Numerical and experimental study of the dynamic thermal resistance of ventilated air-spaces behind passive and active façades, Build. Environ. 225 (2022), https://doi.org/10.1016/j.buildenv.2022.109616.
[80] D.P. Aviram, A.N. Fried, J.J. Roberts, Thermal Properties of a Variable Cavity Wall, 2001 [Online]. Available: www.elsevier.com/locate/buildenv.
[81] A. Pourghorban, B.M. Kari, Evaluation of reflective insulation systems in wall application by guarded hot box apparatus, and comparative investigation with ASHRAE and ISO 15099, Construct. Build. Mater. 207 (2019) 84–97, https://doi.org/10.1016/j.conbuildmat.2019.02.097.

[82] M. Rahiminejad, D. Khovalyg, Thermal resistance of ventilated air-spaces behind external claddings; definitions and challenges (ASHRAE 1759-RP), Sci. Technol. Built. Environ. 27 (6) (2021) 788–805, https://doi.org/10.1080/23744731.2021.1898819.
[83] D. Chowdhury, S. Neogi, Thermal performance evaluation of traditional walls and roof used in tropical climate using guarded hot box, Construct. Build. Mater. 218 (2019) 73–89, https://doi.org/10.1016/j.conbuildmat.2019.05.032.
[84] A. Tadeu, L. Śkerget, N. Simões, R. Fino, Simulation of heat and moisture flow through walls covered with uncoated medium density expanded cork, Build. Environ. 142 (2018) 195–210, https://doi.org/10.1016/j.buildenv.2018.06.009.
[85] K. Ulgen, "Experimental and Theoretical Investigation of Effects of Wall's Thermophysical Properties on Time Lag and Decrement Factor.".
[86] X. Lu, A.M. Memari, Comparative study of Hot Box Test Method using laboratory evaluation of thermal properties of a given building envelope system type, Energy Build. 178 (2018) 130–139, https://doi.org/10.1016/j.enbuild.2018.08.044.
[87] T. Pflug, B. Bueno, M. Siroux, T.E. Kuhn, Potential analysis of a new removable insulation system, Energy Build. 154 (Nov. 2017) 391–403, https://doi.org/10.1016/j.enbuild.2017.08.033.
[88] EN 410, Glass in Building – Determination of Luminous and Solar Characteristics of Glazing, 2011.
[89] ISO 15099: Thermal Performance of Windows, Doors and Shading Devices - Detailed Calculations, 2003.
[90] M. Dabbagh, M. Krarti, Evaluation of the performance for a dynamic insulation system suitable for switchable building envelope, Energy Build. 222 (2020), https://doi.org/10.1016/j.enbuild.2020.110025.
[91] W. Chun, Y.J. Ko, H.J. Lee, H. Han, J.T. Kim, K. Chen, Effects of working fluids on the performance of a bi-directional thermodiode for solar energy utilization in buildings, Sol. Energy 83 (3) (2009) 409–419, https://doi.org/10.1016/j.solener.2008.09.001.
[92] M.Y. Wong, C.Y. Tso, T.C. Ho, H.H. Lee, A review of state of the art thermal diodes and their potential applications, in: International Journal of Heat and Mass Transfer, vol. 164, Elsevier Ltd, 2021, https://doi.org/10.1016/j.ijheatmasstransfer.2020.120607.
[93] R. Tan, Z. Zhang, Heat pipe structure on heat transfer and energy saving performance of the wall implanted with heat pipes during the heating season, Appl. Therm. Eng. 102 (2016) 633–640, https://doi.org/10.1016/j.applthermaleng.2016.03.085.
[94] GB/T13475 Thermal Insulation–Determination of Steady-State Thermal Transmission Properties–Calibrated and Guard Hot Box, 2008.
[95] C. Liu, Z. Zhang, Thermal response of wall implanted with heat pipes: experimental analysis, Renew. Energy 143 (2019) 1687–1697, https://doi.org/10.1016/j.renene.2019.05.123.
[96] A. Pugsley, A. Zacharopoulos, J. Deb Mondol, M. Smyth, Vertical Planar Liquid-Vapour Thermal Diodes (PLVTD) and their application in building façade energy systems, Appl. Therm. Eng. 179 (2020), https://doi.org/10.1016/j.applthermaleng.2020.115641.